Formation of Magnetic Microphases in $Ca_3Co_2O_6$

Y. Kamiya and C. D. Batista

Theoretical Division, T4 and CNLS, Los Alamos National Laboratory, Los Alamos, New Mexico 87545, USA

(Received 8 March 2012; published 8 August 2012)

We study a frustrated quantum Ising model relevant for $Ca_3Co_2O_6$ that consists of a triangular lattice of weakly coupled ferromagnetic chains. According to our quantum Monte Carlo simulations, the chains become ferromagnetic and form a three-sublattice "up-up-down" structure for $T \leq T_{CI}$. In contrast, long-wavelength spin-density-wave microphases are stabilized along the chains for $T_{CI} < T < T_c$. Our mean field solutions reveal a quasicontinuous temperature dependence of the modulation wavelength, implying the existence of metastable states that explain the very slow dynamics observed in $Ca_3Co_2O_6$. We also discuss implications of microphases for the related multiferroic compounds Ca_3CoMnO_6 and Lu_2MnCoO_6.

DOI: 10.1103/PhysRevLett.109.067204 PACS numbers: 75.10.Jm, 75.25.−j, 75.40.Mg

Introduction.—Geometric frustration, low dimensionality, and quantum fluctuations can lead to exotic phase transitions and states of matter [1,2] such as the field-induced magnetization plateaus of $SrCu_2(BO_3)_2$ [3–5], the spin-driven "nematic" transition in pnictides [6–9], and the dimensional reduction in $BaCuSi_2O_6$ [10,11]. $Ca_3Co_2O_6$ is another example comprising a triangular lattice of ferromagnetic (FM) Ising chains coupled by weak antiferromagnetic (AFM) exchanges. This compound exhibits field-induced magnetization steps whose heights depend on the field sweep history and rate [12–16]. We will show that this out-of-equilibrium behavior has its roots in exotic equilibrium properties that can be extended to the related multiferroic compound $Ca_3Co_{2-x}Mn_xO_6$ [17–23].

The Co^{3+} ions (Co II) on the trigonal prism sites of $Ca_3Co_2O_6$ contain $3d^6$ localized electrons that generate an $S = 2$ spin with large Ising-like anisotropy [24–28]. These ions form a triangular lattice of FM Ising chains along the c axis (Fig. 1), and the structure comprises three sublattices of layers stacked along the c axis in an $ABCABC\ldots$ configuration. Although the AFM interchain couplings J_2 and J_3 [29] [Fig. 1(a)] are an order of magnitude smaller than the intrachain FM exchange, $|J_1| = 2 \times 10$ K [24,29], we will show that they strongly affect the intrachain spin correlations over a window of temperatures below T_c.

The initial interest in $Ca_3Co_2O_6$ was triggered by the observation of out-of-equilibrium magnetization steps that appeared at regular field intervals below ~8 K and ~3.6 T. A previous study indicated some similarity to quantum tunneling in molecular magnets [30]. Other studies invoked a "rigid-chain model," in which every chain is replaced by a single Ising spin by assuming $T \ll |J_1|$ [31–35]. Each spin of the resulting triangular lattice Ising model represents the magnetization of the whole chain, and it is flipped if $g\mu_B H$ overcomes its molecular field. Within this simplified framework, regular field intervals result from the equally spaced discrete molecular field spectrum of the triangular lattice Ising model [31]. However, this 2D scenario was challenged by the recent discovery of long-wavelength intrachain spin-density-wave (SDW) ordering below $T_c \simeq 25$ K [16,36,37]. Motivated by this discovery, Chapon initiated the study of a more realistic 3D lattice model by using a random-phase approximation, which is valid only close to $T = T_c$ [38].

By combining the quantum Monte Carlo (QMC) simulations and mean field (MF) solutions of the 3D quantum Ising model relevant for $Ca_3Co_2O_6$, we reproduce most of the measured zero-field properties. A sequence of soliton lattices that lead to the observed SDW order appears for $T_{CI} < T < T_c$ through the competition between intra- and interchain couplings. While the transverse field stabilizes a ferrimagnetic (FIM) up-up-down (UUD) state below T_{CI} via order by disorder [39], very small longer-range exchange couplings, not included in our model, should be responsible for the actual $T = 0$ ordering of $Ca_3Co_2O_6$ [40]. Our MF solutions show that the ordering wave vector changes quasicontinuously as a function of T, implying the existence of many competing metastable states. Although the modulation wavelength increases for a lower T and the rigid-chain picture is apparently applicable for $T < T_{CI}$, the relaxation is known to be extremely slow and

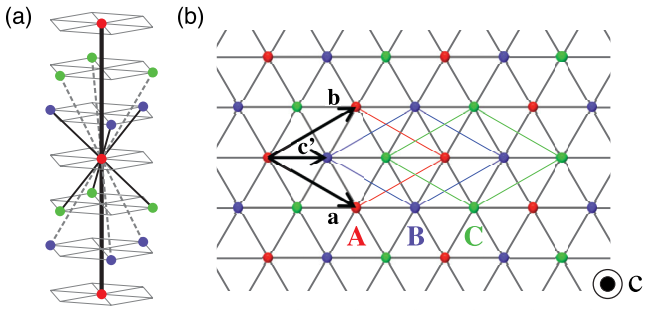

FIG. 1 (color online). (a) Exchange couplings between the Co II ions: The FM coupling J_1 (a thick solid line) and the AFM couplings J_2 (thin solid lines) and J_3 (dash lines). The lines within the layers are projections of the interchain couplings. (b) The lattice projected on the ab plane. Each dot represents a chain.

practically never complete [16]. According to our results, the observed slow dynamics for $T \lesssim 10$ K [16] is a direct consequence of the multiple SDW microphases that appear for $T_{\rm CI} < T < T_c$. This exotic regime can only be captured by solving the 3D model beyond the random-phase approximation [38].

Model.—We use a pseudospin-1/2 to represent the lowest energy doublet ($S^z = \pm 2$) of the Co II ions. The Hamiltonian is [37,38]

$$\mathcal{H} = \sum_{\langle ij \rangle} J_{ij} \sigma_i^z \sigma_j^z - H \sum_i \sigma_i^z - \Gamma \sum_i \sigma_i^x, \qquad (1)$$

where $\boldsymbol{\sigma}_i$ is the vector of Pauli matrices for the ion i on the 3D lattice shown in Fig. 1, $J_{ij} = J_1$ for nearest-neighbor (NN) sites along the chains, and $J_{ij} = J_2(J_3)$ for the NN sites on NN (next-NN) layers [Fig. 1(a)]. Previous measurements indicate that J_1 is FM ($J_1 < 0$), while J_2 and J_3 ($J_2, J_3 \ll |J_1|$) are AFM [14]. $H = g_c \mu_B S B$ is the external magnetic field along the c axis (g_c is the gyromagnetic factor), while the transverse field is included for accelerating the QMC relaxation and removing the macroscopic ground state degeneracy without invoking smaller and unknown longer-range exchange couplings. We will assume $J_2 = J_3 = 0.1|J_1|$, $\Gamma = 0.3|J_1|$, and $H = 0$ unless otherwise specified [41].

We use the continuous-time QMC method [42,43] to compute the thermodynamic phase diagram. There is no sign problem because the frustrated terms are diagonal. The clusters can expand along each chain and the imaginary-time (τ) direction. The weight factors due to J_2 and J_3 appear in the cluster-flip attempt. We use the replica exchange method [44] for the lowest-T simulations [45]. The simulated lattice has $L \times L \times L_c$ unit cells with $L_c = 10L$ ($N_{\rm layer} \equiv 3L_c$ layers).

Figures 2(a) and 2(b) show the specific heat C obtained from our QMC simulations for periodic boundary conditions (PBCs) and open boundary conditions (OBCs) along the c axis, while PBCs are applied in the a and b directions. There are three different regimes. The λ peak at $T_c \simeq 1.4|J_1|$ indicates a 3D phase transition from a paramagnetic phase to an ordered state. In addition, there are two different ordered regimes below T_c separated by a tiny peak at $T \lesssim 0.1|J_1|$, which we will refer to as intermediate- and low-T regimes. While the position of this peak exhibits moderate size dependence, the consistent shift toward higher T for larger values of L implies robustness of the lowest-T phase against size effects. The sensitivity of $C(T)$ to the boundary conditions along the c axis for $T \lesssim T_c$ is caused by a mismatch between the wave vectors of the finite size lattice and the optimal SDW wave vector in the intermediate-T regime. In what follows, we adopt OBCs along the c axis, because it is more convenient for detecting modulations with wavelength comparable to $N_{\rm layer}$ (see below).

FIM state in the low-T regime.—We will first discuss the state of equilibrium in the low-T regime. If $\Gamma = T = 0$, every chain is FM and the ground state subspace has the well-known massive degeneracy of the triangular lattice Ising model [47]. The lowest order correction to the ground state energy is $O(\Gamma^2)$. We introduce the hexagonal plaquette variables $\tau^z_{(\mu)i} \equiv (1/2)\sum_{\langle ij \rangle_\mu} \sigma_j^z$, with $\langle ij \rangle_\mu$ denoting the sites connected by J_μ ($\mu = 2, 3$). Since any unperturbed ground state satisfies $\sigma_i^z \tau^z_{(\mu)i} = -|\tau^z_{(\mu)i}|$ and $\tau^z_{(2)i} = \tau^z_{(3)i} \equiv \tau_i^z$, the energy cost of flipping a spin of the ion i is $\Delta E_i = 4|J_1| + 4\bar{J}|\tau_i^z|$, where $\bar{J} \equiv (J_2 + J_3)/2$. Therefore, the leading nontrivial contribution to the second-order effective Hamiltonian, $\mathcal{H}_2^{\rm eff} = -\sum_i \Gamma^2/\Delta E_i$, is

$$\mathcal{H}_2^{\rm eff} = -\frac{\Gamma^2 \bar{J}^2}{4|J_1|^3} \sum_i |\tau_i^z|^2 + O\left(\frac{\Gamma^2 \bar{J}^3}{|J_1|^4}\right) + \text{const.} \qquad (2)$$

Here, the projection of $\sum_i |\tau_i^z|$ in the unperturbed ground state subspace is a constant. Consequently, the lowest-order nontrivial effective interaction is an FM coupling between the next-NN chains that stabilizes the three-sublattice UUD state of FM chains. This FIM state has a spontaneous magnetization at 1/3 of the saturation value. To verify this numerically, we calculate $\langle |\sigma^z_{\boldsymbol{q}=0,\omega=0}|^2 \rangle = \langle |N^{-1}\beta^{-1} \sum_i \int_0^\beta d\tau \sigma_i^z(\tau)|^2 \rangle$. Figures 2(c) and 2(d) show that $\langle |\sigma^z_{\boldsymbol{q}=0,\omega=0}|^2 \rangle$ approaches $(1/3)^2 = 1/9$ in the low-T regime in agreement with our analytical result. The corresponding ordering temperature coincides with the tiny anomaly in $C(T)$.

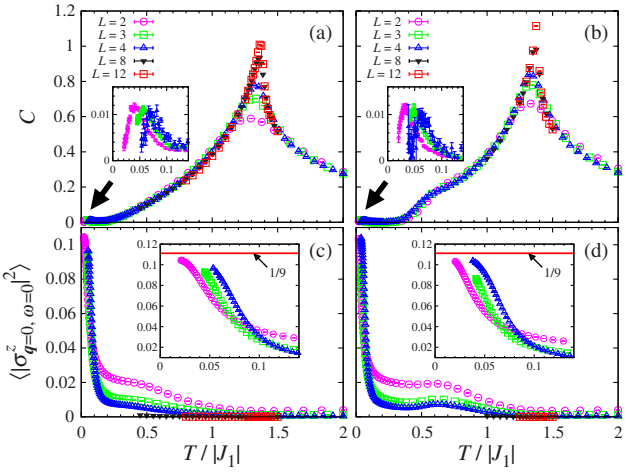

FIG. 2 (color online). The upper panels show the specific heat, while the lower panels show $|\sigma^z_{\boldsymbol{q}=0,\omega=0}|^2$ for $J_2 = J_3 = 0.1|J_1|$ and $\Gamma = 0.3|J_1|$. OBCs (PBCs) are imposed in the c direction in (a) and (c) [(b) and (d)]. The arrows indicate a tiny anomaly in the low-T regime. The insets provide enlarged views.

SDW order in the intermediate-T regime.—We will next discuss the most important intermediate-T regime. Figure 3 shows the equal-time structure factor $S(\boldsymbol{q}) = N^{-1} \sum_{ij} e^{-i\boldsymbol{q}\cdot(\boldsymbol{r}_i - \boldsymbol{r}_j)} \langle \sigma_i^z \sigma_j^z \rangle$ slightly below T_c (at $T = 1.3|J_1|$), which was extracted from the major peak of $C(T)$. The Bragg peak at $q_3 = Q_3$ is slightly shifted from $q_3 = 2\pi/3$, indicating modulated spin ordering along the c axis [Fig. 3(a)], while Fig. 3(b) clearly shows that each

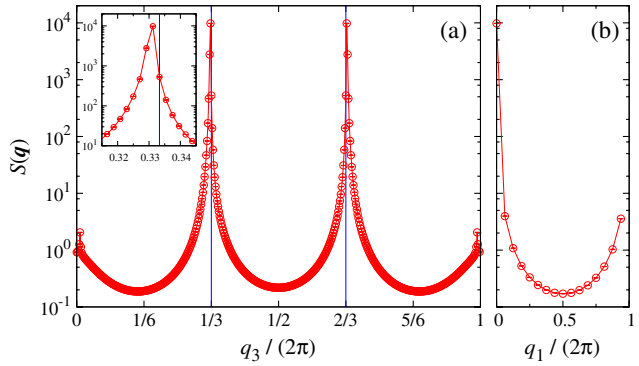

FIG. 3 (color online). $S(\boldsymbol{q})$ at $T = 1.3|J_1|$ for $J_2 = J_3 = 0.1|J_1|$, $\Gamma = 0.3|J_1|$, $L = 16$ ($N_{\text{layer}} = 480$), and OBCs along the c axis. The vertical lines in (a) indicate $q_3 = 2\pi/3$ and $4\pi/3$, and the inset shows an enlarged view around $q_3 = 2\pi/3$. The wave vector is varied as (a) $\boldsymbol{q} = (0, 0, q_3)$ and (b) $\boldsymbol{q} = (q_1, 0, Q_3)$. Error bars are smaller than the symbol size. The line is a guide to the eye.

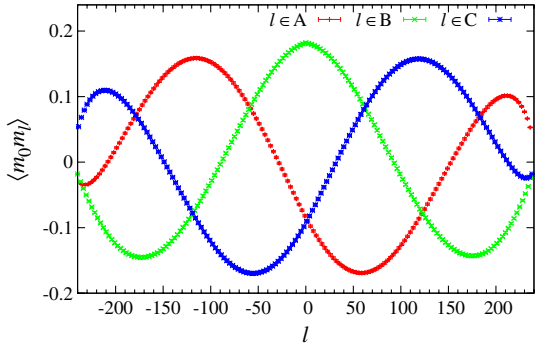

FIG. 4 (color online). $\langle m_0 m_l \rangle$ for the same J_2, J_3, Γ, T, and L as in Fig. 3. Open boundary conditions are imposed in the c direction, and the center layer of the simulated lattice is chosen as $l = 0$.

layer is FM. This is a three-sublattice SDW order with a relative phase shift of $2\pi/3$; the numerical results are consistent with $\langle \sigma^z_{i,\nu} \rangle \approx a \cos(q' r_{i,3} + \phi_\nu)$ ($\nu \in \{A, B, C\}$) in the single-harmonic approximation, where $q' \equiv Q_3 - 2\pi/3$, $r_{i,3}$ is the layer index of site i and $\phi_C - \phi_B = \phi_B - \phi_A = 2\pi/3$. The very small value of $|q'|$ implies that the modulation wavelength is very long: $2\pi|q'|^{-1} \simeq 3 \times 10^2$ at $T = 1.3|J_1|$. These features become even more evident in the correlation functions of average moments per layer $m_l = L^{-2} \sum_{i; r_{i,3} = l} \sigma^z_i$ (Fig. 4). The abrupt decay close to the edges is a consequence of OBCs. Although larger systems are necessary to determine the precise T dependence of q', the obtained long-wavelength modulation is in excellent agreement with recent experiments [16,36,37].

We now discuss the origin of the SDW and note that this ordering does not appear in apparently similar lattices. For example, hexagonal lattice Ising systems, such as $CsCoCl_3$ and $CsCoBr_3$, exhibit the partially disordered AFM state for intermediate T, even though they are also realizations of weakly coupled Ising FM chains that form a triangular lattice [48]. The crucial difference is in the connectivity of the interchain couplings: while the hexagonal lattice contains frustrated loops only within each layer, J_2 and J_3 connect spins on different layers (Fig. 1) and consequently compete against the dominant intrachain coupling J_1.

Our numerical results suggest a natural MF approximation. We assume that each layer is FM, as it is indicated by our QMC simulation. Indeed, the intralayer effective FM coupling is induced not only by Γ but also by thermal fluctuations (it appears in the second-order contribution of a high-T expansion). In fact, our MC simulations show that the microphases still exist over an extended window of temperatures even in the absence of the transverse field. As expected, this phenomenon is entirely driven by the classical exchange interaction between Ising variables on a particular type of geometrically frustrated lattice. Therefore, we will assume $\Gamma = 0$ in what follows. The MF equations for the magnetization of each layer are

$$\langle m_l \rangle = \tanh \beta h_l, \tag{3}$$

with $h_l = -J_1(\langle m_{l+3} \rangle + \langle m_{l-3} \rangle) - 3J_2(\langle m_{l+1} \rangle + \langle m_{l-1} \rangle) - 3J_3(\langle m_{l+2} \rangle + \langle m_{l-2} \rangle)$. The wave-vector Q_c of the highest-T ordered phase is given by the minimum of $J_{\text{MF}}(q) = 2J_1 \cos 3q + 6J_2 \cos q + 6J_3 \cos 2q$, and $T_c = -J_{\text{MF}}(Q_c)$ [38]. If J_2 and J_3 are AFM, any finite interchain coupling leads to incommensurate SDW ordering at $T = T_c$ [38]. The MF solution for $T < T_c$ is obtained by solving Eq. (3) numerically. Figure 5 shows $q'(T) \equiv Q(T) - 2\pi/3$, i.e., the ordering wave vector Q shifted by a constant, obtained by imposing PBCs, and varying N_{layer} up to 2000 ($J_2 = J_3 = 0.1|J_1|$). The $q'(T)$ curve is qualitatively similar to the ones obtained for the ANNNI model [49]. However, we are not aware of any unambiguous realization of this prototypical model in Mott insulators. The $q' = 0$ phase (FM chains) stabilized at the lowest temperatures is the UUD FIM state obtained from our analytical approach and the QMC simulations. This state becomes unstable for $T > T_{\text{CI}} \approx 2.171|J_1|$ (overestimation of T_{CI} is expected for a MF approximation), above which $q'(T)$ changes quasicontinuously. The obtained amplitude $|q'|$ is small in

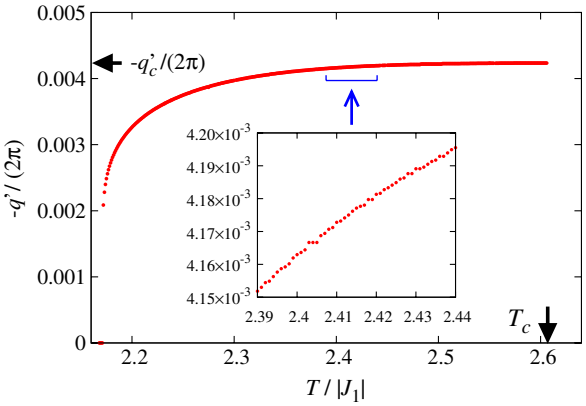

FIG. 5 (color online). $q'(T)$ obtained from the MF theory ($J_2 = J_3 = 0.1|J_1|$). The inset shows an enlarged view.

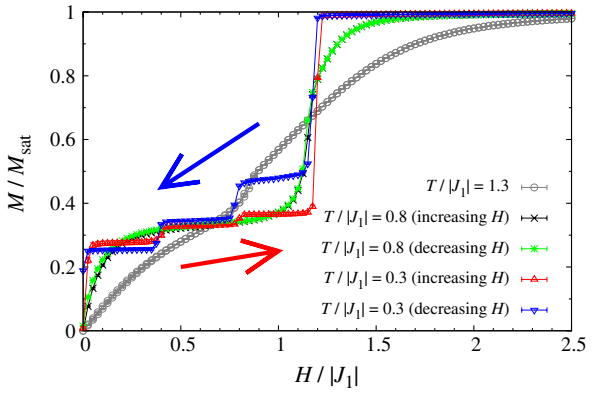

FIG. 6 (color online). Magnetization curve obtained by using a relaxation process described in the text, for $J_2 = J_3 = 0.1|J_1|$, $\Gamma = 0.3|J_1|$, $L = 12$ ($N_{\text{layer}} = 360$), and OBCs in the c direction.

the entire regime, in agreement with experiments in Refs. [16,36,37] and with our QMC results. The optimal states are determined through close competition among many metastable states. This also implies that the fine structure of $q'(T)$ should be very sensitive to small additional couplings that are not included in our model. However, the quasicontinuous change of $q'(T)$ is a robust feature.

A continuum approximation of our MF theory (analogous to Ref. [50]) shows that the SDW phase corresponds to a quasicontinuous sequence of microphases driven by entropic effects stabilizing a finite concentration of solitons (kinks) along the chains. The solitons form domain walls perpendicular to the c axis. They crystallize into a lattice, and the mean separation λ between walls determines $q' \propto \lambda^{-1}$. The value of λ is controlled by a balance between the chemical potential of solitons and an effective repulsive interaction that decays exponentially in the distance between solitons [50]. The outcome of this balance is that λ diverges logarithmically in $T - T_{\text{CI}}$ [our result (Fig. 5) reproduces this behavior]. A number of metastable states appear in this regime with different modulation periods. They are separated by free energy barriers associated with the creation or annihilation and redistribution of magnetic domain walls. These barriers give the dominant contribution to the observed slow dynamics because the relevant relaxation modes are suppressed at sufficiently low temperatures.

Magnetization curve.—Finally, we present $M(H)$ obtained in a simulated relaxation process in the realistic 3D model. We equilibrate the system at a given T for $H = 0$ and then increase H gradually. We take 10^4 steps at each value of H, which is insufficient for equilibration at $T \ll T_c$. After reaching a sufficiently high field, we go back to $H = 0$ in the same way, and stop. For $H \neq 0$, we only allow clusters to expand in the τ direction, which corresponds to a classical single spin flip when $\Gamma = 0$. Although our dynamics is different from the real dynamics, our results reproduce the main experimental observations, except for the less clear steps that appear at the highest fields (above $\sim$3.6 T) [12–16]. As shown in Fig. 6, slightly below T_c ($T = 1.3|J_1|$) we find only a small feature suggesting a 1/3 plateau, which becomes more pronounced at $T = 0.8|J_1|$ accompanied by small hysteresis. Steps at regular magnetic field intervals appear at $T = 0.3|J_1|$, which is still inside the SDW phase for $H = 0$. The reproduction of equidistant steps in the relaxation dynamics supports the notion of metastability of the observed low-T states. The heights of the steps obtained with the 3D model differ from the values obtained with the rigid-chain model [31–35].

Conclusions.—We reproduced the temperature-dependent SDW state that was reported by recent neutron diffraction experiments in $Ca_3Co_2O_6$. More importantly, we showed that the SDW phase arises from a crystallization of domain walls that results in a large number of competing metastable states for $T_{\text{CI}} < T < T_c$. By uncovering these microphases in $Ca_3Co_2O_6$, we explained the origin of the extremely slow relaxation of the Bragg peaks [16]. Disorder-induced pinning of the domain walls that exist in the microphases also provides a natural explanation of the observed linear-T contribution in $Ca_3Co_2O_6$ [51]. Order by disorder induced by a small transverse field leads to a FIM phase in the low-T regime. However, this result does not explain the recent observation of an order-order transition to a different commensurate phase [40]. Therefore, although the FIM state is the ground state of Eq. (1), other subtle perturbations, such as intralayer AFM exchange interactions between next-NN chains, must be included to explain the actual $T = 0$ ordering of $Ca_3Co_2O_6$.

From our results we predict that microphases should also exist in the related multiferroic compounds Lu_2MnCoO_6 [52] and $Ca_3Co_{2-x}Mn_xO_6$ ($x \approx 1$) [17–23]. Since magnetic domain walls carry an internal electric dipole moment in these materials [53], the microphases should be sensitive to an external electric field that introduces a bias between walls with opposite electric polarizations. Indeed, the dielectric constant of both compounds exhibits a broad peak below T_c [19,52]. We propose that this peak arises from the long-wavelength modulation of the electric dipole moments induced by different crystallization of magnetic domain walls (microphases).

We thank S.-W. Cheong and T. Suzuki for the valuable discussions. The numerical work was done on the supercomputers of NERSC. Work at LANL was performed under the auspices of the U.S. DOE Contract No. DE-AC52-06NA25396 through the LDRD program.

[1] *Introduction to Frustrated Magnetism: Materials, Experiments, Theory*, edited by C. Lacroix, P. Mendels, and F. Mila (Springer-Verlag, Berlin, 2011).

[2] *Frustrated Spin Systems*, edited by H. Diep (World Scientific, Singapore, 2004).

[3] H. Kageyama, K. Yoshimura, R. Stern, N. V. Mushnikov, K. Onizuka, M. Kato, K. Kosuge, C. P. Slichter, T. Goto, and Y. Ueda, Phys. Rev. Lett. **82**, 3168 (1999).

[4] K. Kodama, M. Takigawa, M. Horvatic, C. Berthier, H. Kageyama, Y. Ueda, S. Miyahara, F. Becca, and F. Mila, Science **298**, 395 (2002).

[5] S. E. Sebastian, N. Harrison, P. Sengupta, C. D. Batista, S. Francoual, E. Palm, T. Murphy, N. Marcano, H. A. Dabkowska, and B. D. Gaulin, Proc. Natl. Acad. Sci. U.S.A. **105**, 20157 (2008).

[6] C. Xu, M. Müller, and S. Sachdev, Phys. Rev. B **78**, 020501(R) (2008).

[7] C. Fang, H. Yao, W.-F. Tsai, J.-P. Hu, and S. A. Kivelson, Phys. Rev. B **77**, 224509 (2008).

[8] Y. Kamiya, N. Kawashima, and C. D. Batista, Phys. Rev. B **84**, 214429 (2011).

[9] R. M. Fernandes, A. V. Chubukov, J. Knolle, I. Eremin, and J. Schmalian, Phys. Rev. B **85**, 024534 (2012).

[10] S. E. Sebastian, N. Harrison, C. D. Batista, L. Balicas, M. Jaime, P. A. Sharma, N. Kawashima, and I. R. Fisher, Nature (London) **441**, 617 (2006).

[11] C. D. Batista, J. Schmalian, N. Kawashima, P. Sengupta, S. E. Sebastian, N. Harrison, M. Jaime, and I. R. Fisher, Phys. Rev. Lett. **98**, 257201 (2007).

[12] H. Kageyama, K. Yoshimura, K. Kosuge, H. Mitamura, and T. Goto, J. Phys. Soc. Jpn. **66**, 1607 (1997).

[13] H. Kageyama, K. Yoshimura, K. Kosuge, M. Azuma, M. Takano, H. Mitamura, and T. Goto, J. Phys. Soc. Jpn. **66**, 3996 (1997).

[14] A. Maignan, C. Michel, A. C. Masset, C. Martin, and B. Raveau, Eur. Phys. J. B **15**, 657 (2000).

[15] V. Hardy, M. R. Lees, O. A. Petrenko, D. McK. Paul, D. Flahaut, S. Hébert, and A. Maignan, Phys. Rev. B **70**, 064424 (2004).

[16] T. Moyoshi and K. Motoya, J. Phys. Soc. Jpn. **80**, 034701 (2011).

[17] Y. J. Choi, H. T. Yi, S. Lee, Q. Huang, V. Kiryukhin, and S.-W. Cheong, Phys. Rev. Lett. **100**, 047601 (2008).

[18] T. Lancaster, S. J. Blundell, P. J. Baker, H. J. Lewtas, W. Hayes, F. L. Pratt, H. T. Yi, and S.-W. Cheong, Phys. Rev. B **80**, 020409 (2009).

[19] Y. J. Jo, S. Lee, E. S. Choi, H. T. Yi, W. Ratcliff, Y. J. Choi, V. Kiryukhin, S. W. Cheong, and L. Balicas, Phys. Rev. B **79**, 012407 (2009).

[20] V. Kiryukhin, S. Lee, W. Ratcliff, Q. Huang, H. T. Yi, Y. J. Choi, and S.-W. Cheong, Phys. Rev. Lett. **102**, 187202 (2009).

[21] R. Flint, H.-T. Yi, P. Chandra, S.-W. Cheong, and V. Kiryukhin, Phys. Rev. B **81**, 092402 (2010).

[22] Z. W. Ouyang, N. M. Xia, Y. Y. Wu, S. S. Sheng, J. Chen, Z. C. Xia, L. Li, and G. H. Rao, Phys. Rev. B **84**, 054435 (2011).

[23] H. Wu, T. Burnus, Z. Hu, C. Martin, A. Maignan, J. C. Cezar, A. Tanaka, N. B. Brookes, D. I. Khomskii, and L. H. Tjeng, Phys. Rev. Lett. **102**, 026404 (2009).

[24] S. Aasland, H. Fjellvåg, and B. C. Hauback, Solid State Commun. **101**, 187 (1997).

[25] E. V. Sampathkumaran, N. Fujiwara, S. Rayaprol, P. K. Madhu, and Y. Uwatoko, Phys. Rev. B **70**, 014437 (2004).

[26] K. Takubo, T. Mizokawa, S. Hirata, J.-Y. Son, A. Fujimori, D. Topwal, D. D. Sarma, S. Rayaprol, and E.-V. Sampathkumaran, Phys. Rev. B **71**, 073406 (2005).

[27] T. Burnus, Z. Hu, M. W. Haverkort, J. C. Cezar, D. Flahaut, V. Hardy, A. Maignan, N. B. Brookes, A. Tanaka, H. H. Hsieh, H.-J. Lin, C. T. Chen, and L. H. Tjeng, Phys. Rev. B **74**, 245111 (2006).

[28] H. Wu, M. W. Haverkort, Z. Hu, D. I. Khomskii, and L. H. Tjeng, Phys. Rev. Lett. **95**, 186401 (2005).

[29] R. Frésard, C. Laschinger, T. Kopp, and V. Eyert, Phys. Rev. B **69**, 140405 (2004).

[30] A. Maignan, V. Hardy, S. Hébert, M. Drillon, M. R. Lees, O. Petrenko, D. McK. Paul, and D. Khomskii, J. Mater. Chem. **14**, 1231 (2004).

[31] Y. B. Kudasov, Phys. Rev. Lett. **96**, 027212 (2006).

[32] X. Yao, S. Dong, H. Yu, and J. Liu, Phys. Rev. B **74**, 134421 (2006).

[33] Y. B. Kudasov, A. S. Korshunov, V. N. Pavlov, and D. A. Maslov, Phys. Rev. B **78**, 132407 (2008).

[34] R. Soto, G. Martínez, M. N. Baibich, J. M. Florez, and P. Vargas, Phys. Rev. B **79**, 184422 (2009).

[35] M. H. Qin, K. F. Wang, and J. M. Liu, Phys. Rev. B **79**, 172405 (2009).

[36] S. Agrestini, C. Mazzoli, A. Bombardi, and M. R. Lees, Phys. Rev. B **77**, 140403 (2008).

[37] S. Agrestini, L. C. Chapon, A. Daoud-Aladine, J. Schefer, A. Gukasov, C. Mazzoli, M. R. Lees, and O. A. Petrenko, Phys. Rev. Lett. **101**, 097207 (2008).

[38] L. C. Chapon, Phys. Rev. B **80**, 172405 (2009).

[39] J. Villain, R. Bidaux, J. P. Carton, and R. Conte, J. Phys. (Paris) **41**, 1263 (1980); Y. Kamiya, N. Kawashima, and C. D. Batista, J. Phys. Soc. Jpn. **78**, 094008 (2009).

[40] S. Agrestini, C. L. Fleck, L. C. Chapon, C. Mazzoli, A. Bombardi, M. R. Lees, and O. A. Petrenko, Phys. Rev. Lett. **106**, 197204 (2011).

[41] $J_2/|J_1|$ and $J_3/|J_1|$ are reasonable choices for $Ca_3Co_2O_6$ and $J_2 = J_3$ does not imply higher symmetry. Γ should be sufficiently smaller than the major exchange coupling $|J_1|$.

[42] H. Rieger and N. Kawashima, Eur. Phys. J. B **9**, 233 (1999).

[43] N. Kawashima and K. Harada, J. Phys. Soc. Jpn. **73**, 1379 (2004).

[44] K. Hukushima and K. Nemoto, J. Phys. Soc. Jpn. **65**, 1604 (1996).

[45] The probability for exchanging two replicas (T_i, Γ_i) and (T_j, Γ_j) is $p_{ij} = \min\{1, \exp(\Delta\beta\Delta E_d)[(\beta_j\Gamma_j)/(\beta_i\Gamma_i)]^{\Delta N_k}\}$ with $\Delta\beta \equiv 1/T_i - 1/T_j$. $\Delta E_d \equiv E_{d,i} - E_{d,j}$ ($\Delta N_k \equiv N_{k,i} - N_{k,j}$) is the difference of the diagonal term (total number of kinks in the τ direction). See also Ref. [46]

[46] H. Ishizuka, Y. Motome, N. Furukawa, and S. Suzuki, Phys. Rev. B **84**, 064120 (2011).

[47] G. H. Wannier, Phys. Rev. **79**, 357 (1950).

[48] M. F. Collins and O. A. Petrenko, Can. J. Phys. **75**, 605 (1997).

[49] P. Bak, Rep. Prog. Phys. **45**, 587 (1982); W. Selke, Phys. Rep. **170**, 213 (1988).

[50] P. Bak and J. von Boehm, Phys. Rev. B **21**, 5297 (1980).

[51] V. Hardy, S. Lambert, M. R. Lees, and D. McK. Paul, Phys. Rev. B **68**, 014424 (2003).

[52] S. Yáñez-Vilar, E. D. Mun, V. S. Zapf, B. G. Ueland, J. S. Gardner, J. D. Thompson, J. Singleton, M. Sánchez-Andújar, J. Mira, N. Biskup, M. A. Señarís-Rodríguez, and C. D. Batista, Phys. Rev. B **84**, 134427 (2011).

[53] S. Cheong and M. Mostovoy, Nature Mater. **6**, 13 (2007).